Changes in the Arctic Ocean CO_2 sink (1996–2007): A regional model analysis

M. Manizza,[1,2] M. J. Follows,[1] S. Dutkiewicz,[1] D. Menemenlis,[3] C. N. Hill,[1] and R. M. Key[4]

Received 20 August 2012; revised 4 October 2013; accepted 11 October 2013; published 19 November 2013.

[1] The rapid recent decline of Arctic Ocean sea ice area increases the flux of solar radiation available for primary production and the area of open water for air-sea gas exchange. We use a regional physical-biogeochemical model of the Arctic Ocean, forced by the National Centers for Environmental Prediction/National Center for Atmospheric Research atmospheric reanalysis, to evaluate the mean present-day CO_2 sink and its temporal evolution. During the 1996–2007 period, the model suggests that the Arctic average sea surface temperature warmed by 0.04°C a^{-1}, that sea ice area decreased by $\sim 0.1 \times 10^6$ km^2 a^{-1}, and that the biological drawdown of dissolved inorganic carbon increased. The simulated 1996–2007 time-mean Arctic Ocean CO_2 sink is 58 ± 6 Tg C a^{-1}. The increase in ice-free ocean area and consequent carbon drawdown during this period enhances the CO_2 sink by ~ 1.4 Tg C a^{-1}, consistent with estimates based on extrapolations of sparse data. A regional analysis suggests that during the 1996–2007 period, the shelf regions of the Laptev, East Siberian, Chukchi, and Beaufort Seas experienced an increase in the efficiency of their biological pump due to decreased sea ice area, especially during the 2004–2007 period, consistent with independently published estimates of primary production. In contrast, the CO_2 sink in the Barents Sea is reduced during the 2004–2007 period due to a dominant control by warming and decreasing solubility. Thus, the effect of decreasing sea ice area and increasing sea surface temperature partially cancel, though the former is dominant.

Citation: Manizza, M., M. J. Follows, S. Dutkiewicz, D. Menemenlis, C. N. Hill, and R. M. Key (2013), Changes in the Arctic Ocean CO_2 sink (1996–2007): A regional model analysis, *Global Biogeochem. Cycles*, *27*, 1108–1118, doi:10.1002/2012GB004491.

1. Introduction

[2] The Arctic Ocean (nominally all the ocean area north of 65°N) and its surrounding land masses have shown the most evident response to recent climate change. Arctic Ocean sea surface temperature has increased [*Steele et al.*, 2008], sea ice thickness has decreased [*Rothrock et al.*, 2008; *Giles et al.*, 2008], and sea ice area has declined [*Stroeve et al.*, 2007], especially during the summer months. In particular, sea ice area experienced a drastic reduction during the last three decades, culminating with a minimum area of 2.9×10^6 km^2 at the end of the boreal summer of 2007, 47%, less than in 1980.

[3] Arctic Ocean sea ice area is an important factor for pelagic marine ecosystems and for biogeochemical processes because it regulates the amount of solar radiation available for phytoplankton primary production and the area of open water available for air-sea gas exchange. For example, it has been estimated that from 1998 to 2006, the primary production (PP) of the entire Arctic Ocean increased by 12×10^7 g C a^{-1} due to the decline of the sea ice area [*Pabi et al.*, 2008]. *Li et al.* [2009] found detectable changes in the Arctic Ocean pelagic ecosystem caused by sea ice melt, upper ocean freshening, and enhanced stratification, inducing an increase in smaller phytoplankton cells, suited to stratified ocean conditions, relative to larger diatoms. *Kahru et al.* [2011] used satellite-derived maps of surface chlorophyll *a* concentration to show significant trends toward earlier phytoplankton blooms in some regions of the Arctic Ocean. Using a physical-ecological model of the Arctic Ocean, *Zhang et al.* [2011] consistently estimated a 50% PP increase in two decades because of declining sea ice area. Evaluations of the current Arctic Ocean CO_2

[1]Program in Atmospheres, Oceans, and Climate, Department of Earth, Atmospheric and Planetary Sciences, Massachusetts Institute of Technology, Cambridge, Massachusetts, USA.
[2]Now at Geosciences Research Division, Scripps Institution of Oceanography, University of California, San Diego, La Jolla, California, USA.
[3]Jet Propulsion Laboratory, California Institute of Technology, Pasadena, California, USA.
[4]Program in Atmosphere and Ocean Sciences, Department of Geosciences, Princeton University, Princeton, New Jersey, USA.

Corresponding author: M. Manizza, Geosciences Research Division, Scripps Institution of Oceanography, University of California, San Diego, 9500 Gilman Dr., La Jolla, CA 92093, USA. (mmanizza@ucsd.edu)

0886-6236/13/10.1002/2012GB004491

sink have significant uncertainties, with recent estimates of 20–100 Tg C a^{-1} [*McGuire et al.*, 2009] to 66–199 Tg C a^{-1} [*Bates and Mathis*, 2009] and 118 ± 7 Tg C a^{-1} [*Arrigo et al.*, 2011], based on interpretations and extrapolations of in situ and remotely sensed data. *Bates et al.* [2006] estimated that during the last three decades, Arctic Ocean CO_2 uptake might have increased from 24 to 66 Tg C a^{-1} because of the progressive decline of sea ice area observed from space.

[4] The scarcity of direct observations, and a desire to understand and predict Arctic Ocean ecosystem changes, motivates the development and utilization of numerical physical-biogeochemical models. Here we describe and use a numerical model that explicitly represents both the physical processes of the ocean and sea ice and the biogeochemical processes that determine the air-sea fluxes of CO_2 in order to assess recent changes in the Arctic Ocean CO_2 sink. We aim to address the following questions:

[5] 1. What was the average CO_2 sink in the Arctic Ocean during the 1996–2007 period?

[6] 2. What was the response of the Arctic Ocean CO_2 sink to climate variability during the 1996–2007 period?

[7] 3. What was the response of the Arctic Ocean CO_2 sink to the two events of sea ice area drastic reduction and ocean warming in 2005 and 2007?

2. Methods

2.1. Regional Arctic Ocean Sea Ice Model

[8] This study is based on a regional Arctic Ocean configuration of the Massachusetts Institute of Technology general circulation model (MITgcm) [*Marshall et al.*, 1997] as described in detail in *Losch et al.* [2010] and previously used in the studies of *Condron et al.* [2009], *Manizza et al.* [2009, 2011], and *Nguyen et al.* [2009, 2011]. The model has 50 vertical levels that vary from 10 m near the surface to 450 m near the ocean bottom, horizontal grid spacing of 18 km, and open boundaries at approximately 55°N in the Atlantic and Pacific sectors. Surface boundary conditions are calculated using the simulated ocean surface state (temperature and sea ice) and a prescribed atmospheric state (2 m air temperature and humidity, 10 m wind velocity, precipitation, and downward longwave and shortwave radiation) from the National Centers for Environmental Prediction (NCEP)/National Center for Atmospheric Research (NCAR) atmospheric reanalysis [*Kalnay et al.*, 1996]. Over open ocean, air-sea fluxes are computed using the bulk parametrization of *Large and Yeager* [2004]. A coupled dynamic/thermodynamic sea ice model [*Losch et al.*, 2010; *Heimbach et al.*, 2010] computes the evolution of sea ice cover area and thickness according to the imposed atmospheric forcing and the physical state of the underlying ocean. The ocean model is initialized with the World Ocean Circulation Experiment global hydrographic climatology [*Gouretski and Koltermann*, 2004]. Sea ice initial conditions are from the Pan-Arctic Ice-Ocean Modeling and Assimilation System [*Zhang and Rothrock*, 2003]. The model is integrated for the period 1992–2007, but this analysis focuses on the 1996–2007 period in order to avoid the strongest upper ocean initialization transients.

2.2. Ocean Biogeochemical Model

[9] The MITgcm ocean and sea ice model is coupled to a simplified biogeochemical model, building on the work of *McKinley et al.* [2004], that simulates the evolution of six tracers: dissolved inorganic carbon (DIC), alkalinity (ALK), dissolved oxygen (O_2), dissolved organic phosphorus, phosphate (PO_4), and riverine dissolved organic carbon (RDOC) (described in detail in *Manizza et al.* [2009, 2011]).

[10] In our model, the biological production organic matter (B) is computed according to a simplified scheme as follows:

$$B = \alpha \frac{I}{I + K_I} \frac{PO_4}{PO_4 + K_{PO_4}} \quad (1)$$

where α = 0.5 μM P $month^{-1}$ is the maximum net community production and the half-saturation constants are K_I = 30 W m^{-2} and K_{PO_4} = 0.5 μM.

[11] This simplified scheme has been successfully used in several modeling biogeochemical studies based on the use of MITgcm [*Verdy et al.*, 2007; *Manizza et al.*, 2011; *Lauderdale et al.*, 2013] in different physical configurations. In our model, the remineralization of RDOC impacts the air-sea fluxes of CO_2 (and hence the ocean carbon uptake) due the explicit coupling of or the marine and terrestrial carbon cycles as shown in our previous study [*Manizza et al*., 2011].

[12] The initial field of PO_4 was taken from finale states of the previous model runs performed by using the Darwin model [*Follows et al.*, 2007] run in the same physical framework and initialized with World Ocean Atlas (WOA) 2005 [*Garcia et al.*, 2006]. Initial fields for DIC and ALK were developed using empirical relationships between those variables and potential temperature and salinity in observed vertical profiles (as described in *Manizza et al.* [2011]). Initial fields of RDOC were taken from previously published simulations [*Manizza et al.*, 2009]. We generated boundary conditions for PO_4 from the WOA 2005 to impose at limits of our model domain PO_4 fields while we used the temperature and salinity fields (used for the physical boundary conditions) to infer the DIC and ALK boundary conditions by using the same empirical relationships used for the initial conditions of the same variables as explained above and used in our previous work [*Manizza et al.*, 2011]. We impose a time-varying partial pressure of atmospheric CO_2, which increases from approximately 354 to 386 ppm during the 1992–2007 simulation period, based on monthly averages from NOAA's Earth System Research Laboratory (http://www.esrl.noaa.gov/gmd/ccgg/trends/). Though the simulation begins in 1992, we analyze results from the period 1996 to 2007, to avoid some initial transients. The simulations of the present-day distributions of the key biogeochemical tracers were discussed in *Manizza et al.* [2011].

3. Results

[13] For this study, we not only carry out an analysis of the pan-Arctic region (north of 65°N) but we also examine variations in nine Arctic Ocean sectors (Figure 1): (1) the Greenland Sea, (2) the Barents Sea, (3) the Kara Sea, (4) the Laptev Sea, (5) the East Siberian Sea, (6) the Chukchi Sea, (7) the Beaufort Sea, (8) the Canadian Archipelago including Baffin Bay, and (9) the central Arctic (all the ocean area north of 82°N).

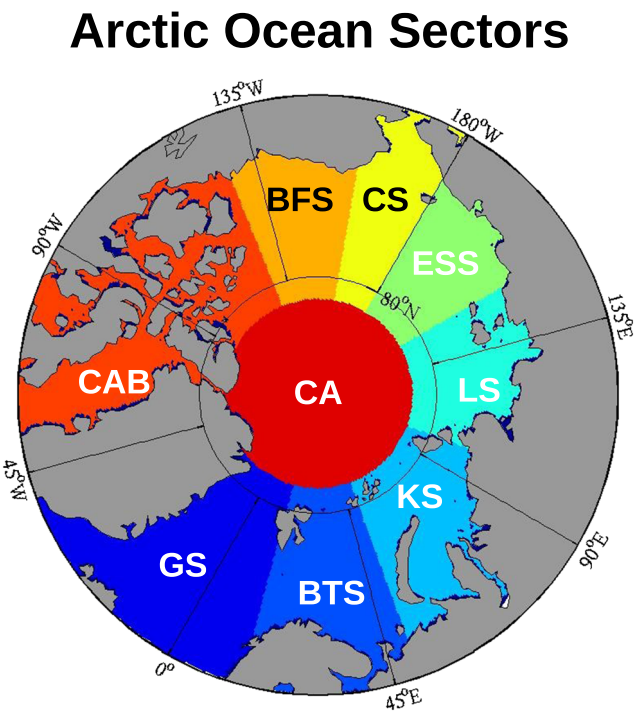

Figure 1. Map of the Arctic Ocean divided in the selected sectors for the regional analysis. GS = Greenland Sea, BTS = Barents Sea, KS = Kara Sea, LS = Laptev Sea, ESS = East Siberian Sea, CS = Chukchi Sea, BFS = Beaufort Sea, CAB = Canadian Archipelago and Baffin Bay, and CA = Central Arctic.

3.1. Sea Surface Temperature (SST) and Sea Ice Area Variability

[14] We start by characterizing the temporal variability of two key physical drivers: SST and sea ice area.

[15] During the 1996–2007 period, the simulated annual average SST shows a clear warming trend (0.04°C a^{-1}), increasing from ∼ -0.5°C to ∼0°C (Figure 2, right, fifth panel, blue line). The simulated SST is compared to the blended SST analysis of *Reynolds et al.* [2007], which shows similar warming trends as those of the simulation (Figure 2, right, fifth panel, red line). This model-data comparison shows that the numerical model is able to realistically reproduce observed interannual SST fluctuations during the 1996–2007 period. Note that there are very few direct observations of SST under sea ice. Therefore, in sea ice-covered regions, a bias between simulation and the *Reynolds et al.* [2007] analysis is to be expected: Simulated SST under sea ice is based on the salinity-dependent freezing point of sea water while the *Reynolds et al.* [2007] analysis uses a sea ice concentration-dependent algorithm as a proxy for under-ice SST. Figure 2 also shows a progressive warming in the individual Arctic Ocean sectors, for example, the Barents, Kara, Laptev, and East Siberian Seas. These regional warming trends generally coincide with a reduction in sea ice area (Figure 3).

[16] The SST warming is accompanied by a progressive reduction of sea ice thickness and of the area of the ocean covered by sea ice. In the annual average, the simulated oceanic area covered by sea ice is equal to ∼10 × 10^6 km^2 in 1996, and it is reduced by 9.2 × 10^6 km^2 in 2007 (Figure 3, right, fifth panel). In order to evaluate the realism of the physical model, we compared simulated sea ice concentration to observations (Figure 3). Satellite data of sea ice concentration from the bootstrap technique [*Comiso et al.*, 1997] was obtained on a 25 km horizontal grid from the National Snow and Ice Data Center. The data-model comparison shows that our model captures fairly realistically the interannual variations of the sea ice area although our model (blue line) tends to overestimate the data values (red line) in all the selected regions except in the central Arctic Ocean. This data-model discrepancy occurs primarily during the melt season, except in the Greenland Sea where the discrepancy is primarily during winter months and advective in nature. The main causes of the differences between simulated and observed sea ice concentration are discussed in *Nguyen et al.* [2011] and will not be further investigated in this study.

[17] Figure 2 also shows a progressive warming in the individual Arctic Ocean sectors, for example, the Barents, Kara, Laptev, and East Siberian Seas. These regional warming trends generally coincide with a reduction in sea ice area (Figure 3) although our model seems to underestimate the observed SST values.

3.2. Variability of Biological Production

[18] In part, temporal variability of the oceanic CO_2 sink is driven by the variability of primary production during the phytoplankton growing season [*Le Quéré et al.*, 2003] modulated in the Arctic Ocean by the extent of the sea ice area which modulates the light available to support the photosynthetic activity [*Pabi et al.*, 2008; *Arrigo et al.*, 2008]. Our simplified biogeochemical model does not explicitly compute primary production, and we evaluate surface Net Community Production (sNCP) as a metric of the biological pump and its interannual variations. A similar approach has

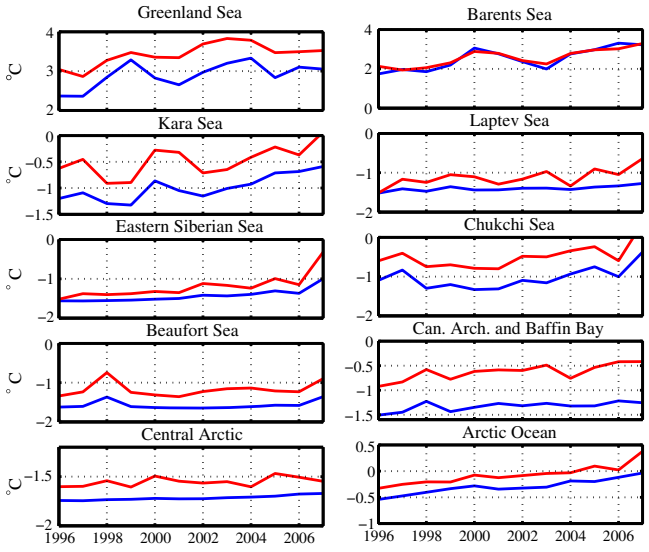

Figure 2. Temporal changes of the annual average of SST during the 1996–2007 period for the sectors of Figure 1 and for the entire Arctic Basin. Blue and red lines indicate model results and satellite-derived data, respectively. Units are °C.

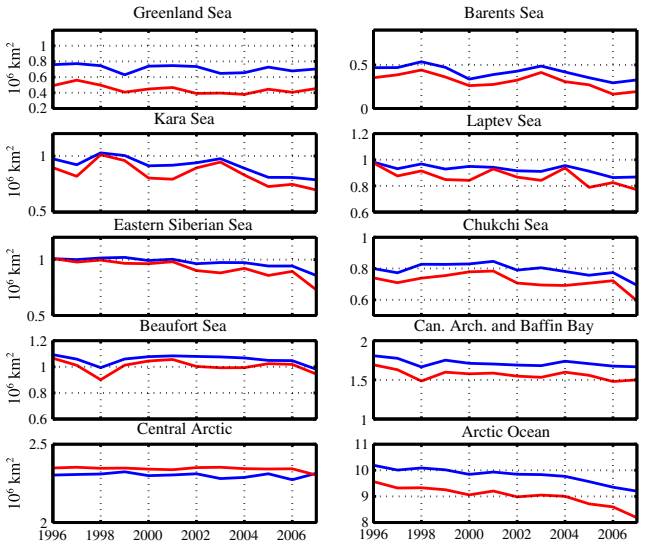

Figure 3. Temporal changes of the annual average of sea ice area during the 1996–2007 period for the sectors of Figure 1 and for the entire Arctic Basin. Blue and red lines indicate model results and satellite-derived data, respectively. Units are km^2.

been also been taken with in situ observations in the surface ocean given that in the Arctic Ocean, autotrophic processes dominate over heterotrophic respiration [*Bates*, 2006] during the phytoplankton growing season, hence promoting a net carbon influx into the surface Arctic waters.

[19] Integrated over the entire Arctic Ocean, there is a clear increasing trend in simulated sNCP (Figure 4, fifth panel), accelerated during the period 2004–2006, due to the notable reduction in sea ice cover. This temporal trend in modeled sNCP is qualitatively consistent with the basin-scale increase in primary production evaluated from remotely sensed data over the same period by *Pabi et al.* [2008]. (A direct comparison is not possible since the model does not resolve primary producers.) A finer scale, regional analysis reveals some interesting patterns: In the period 2004–2007, the simulated Kara Sea, East Siberian Sea, and Chukchi Sea exhibit a clear increase in modeled sNCP (Figure 4). This is also qualitatively consistent with the increase in PP inferred by *Pabi et al.* [2008] in those regions. In the case of Barents Sea, both modeled sNCP and satellite-derived PP estimates also show the same trend of increase although with some disagreement during 2001 and 2002.

[20] In the Laptev Sea, however, our model predicts an increase in sNCP (Figure 4, right, second panel) due to sea ice area reduction (Figure 3). Here the satellite-derived estimates of PP [*Pabi et al.*, 2008] do not show the same clear change.

3.3. Carbon Pumps and CO_2 Sink Variability

[21] While changes in sea ice area drive variations of sNCP and the biological carbon pumps, changes in SST affect the efficiency of the solubility pump of carbon. We evaluate and separate the changes in modeled, surface ocean pCO_2 due to changes in SST and other processes using the method of *Takahashi et al.* [2002] also adopted by *McKinley et al.* [2006]. We calculate the pCO_2 value depending on changes in SST (pCO_2-SST) in the following way:

$$pCO_2\text{-SST} = pCO_2^* \cdot e^{[a\cdot(\text{SST}-\text{SST}^*)]} \quad (2)$$

$$pCO_2\text{-nonSST} = pCO_2 \cdot e^{[a\cdot(\text{SST}^*-\text{SST})]} \quad (3)$$

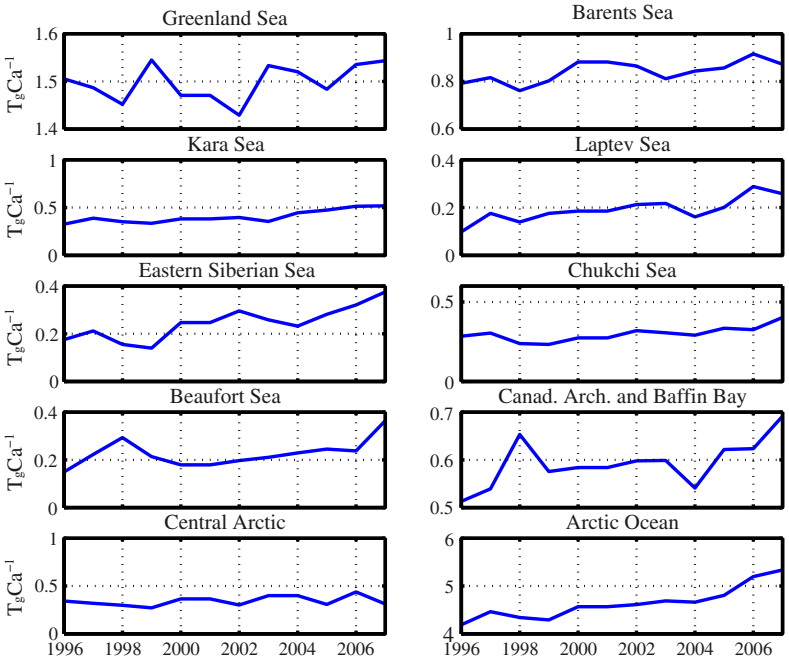

Figure 4. Temporal changes of annual average of surface NCP integrated for nine sectors of the Arctic Ocean and for the Arctic Basin for the 1996–2007 period. Units are Tg C a^{-1}.

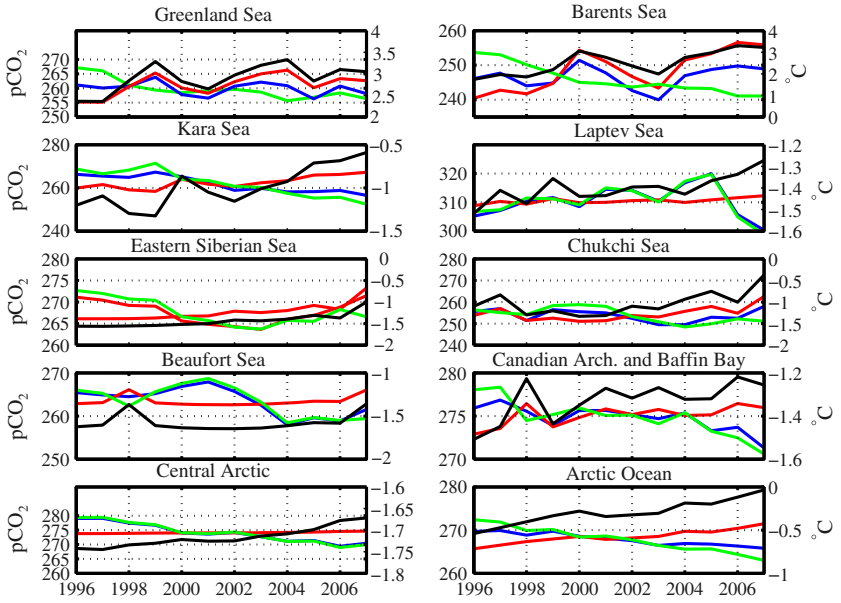

Figure 5. Temporal evolution of the (blue) total, (red) thermal, and (green) nonthermal components (including biologically driven processes) of surface ocean pCO_2 for both nine selected sectors of the Arctic Ocean and for the entire Arctic Basin for the 1996–2007 period. Black line indicates the temporal evolution of SST. Values indicate annual average, and units are μatm and °C for surface ocean pCO_2 and SST, respectively.

where $a = 0.0423$ μatm °C^{-1}, pCO_2^* and SST* are pCO_2 and SST values averaged over the 1996–2007 period while SST and pCO_2 are the time-varying values. The non-SST-driven changes reflect a combination of mechanisms including the biological processes with some potential contribution from entrainment and circulation. The separation of the two components reveals that the nine selected sectors of the Arctic Ocean show different responses to the progressive Arctic climate warming.

[22] In the Greenland Sea and Barents Sea, the changes in the solubility pump (red line) dictated by the SST variability dominate the changes in surface ocean pCO_2 (blue), although in both sectors there is a progressive increase in the efficiency of the biological pump (green line) as pCO_2 is decreased (Figure 5, first panels) following the reduction in sea ice area.

[23] In the Eurasian sector, the reduction of surface pCO_2 is evident for the Kara and the Laptev Seas (Figure 5) where the variability of sea ice area directly drives the biological drawdown of CO_2. This pattern is consistent with the trend derived from the satellite-based observations [*Rodrigues*, 2008] although the time period simulated here is shorter. In the East Siberian, Beaufort, and Chukchi Seas (Figure 5), the total surface ocean pCO_2 (blue line) is mostly driven by the variations in the biological pump (green line) for most of the simulation although in the last year (2007) the abrupt SST warming promotes a clear switch to the dominance of the solubility pump (red line) over the biological pump.

[24] In the Canadian Archipelago and Baffin Bay sector, the year 2004 corresponds to a switch between dominance of the biological and solubility pumps: After 2004, the biological pump dominates while prior to 2004 neither solubility nor biological forcing clearly dominates. In the Central Arctic surface waters, total surface ocean pCO_2 (blue line) reduction is driven by the progressive decrease in DIC caused by the increasing efficiency of the biological pump (green line) (Figure 5) due to the reduction in sea ice area.

[25] If we consider the entire Arctic Ocean (≥ 65°N), the surface pCO_2 decomposition shows a clear divergence in the trend of the biological and solubility pumps with a dominance of the first given that the resulting trend is a net and progressive decrease of the surface ocean pCO_2 (blue line) from 270 to 265 μatm (Figure 5, right, fifth panel).

[26] Changes in surface ocean pCO_2 in the selected locations of the Arctic Ocean directly drive temporal variations in the CO_2 sink for the 1996–2007 period. The sea ice area reduction causes an increase in the CO_2 sink of the Kara Sea that has its own maximum value in 2006 (∼10 Tg C a^{-1}, Figure 6). In the East Siberian, Chukchi, and Beaufort Seas, however, the progressive increase in CO_2 oceanic sink culminates in 2007 (Figure 6) and corresponds to the second and more drastic reduction in sea ice area with values of oceanic CO_2 sink of ∼1.3, ∼3, and ∼2 Tg C a^{-1}, respectively. The Beaufort Sea shows an increase in the oceanic CO_2 sink during the final part of the simulation (2004–2007) driven by the reduction of sea ice area showing a clear dominance of the perturbation of biological pump over the solubility pump (Figure 6, left, fourth panel).

[27] Looking at the basin-scale change, the simulated Arctic Ocean CO_2 sink shows an increase from ∼50 Tg C yr^{-1} (1996) to 65 Tg C a^{-1} (2007) with an average CO_2 sink of 58±6 Tg C a^{-1} (Figure 6, right, fifth panel). It is interesting to note that the maximum CO_2 sink occurs in the year 2005 although the decrease in sea ice area is larger in 2007 than 2005. This would suggest that transitioning from 2004 to 2005, the drastic reduction in sea ice area (Figure 3) boosts

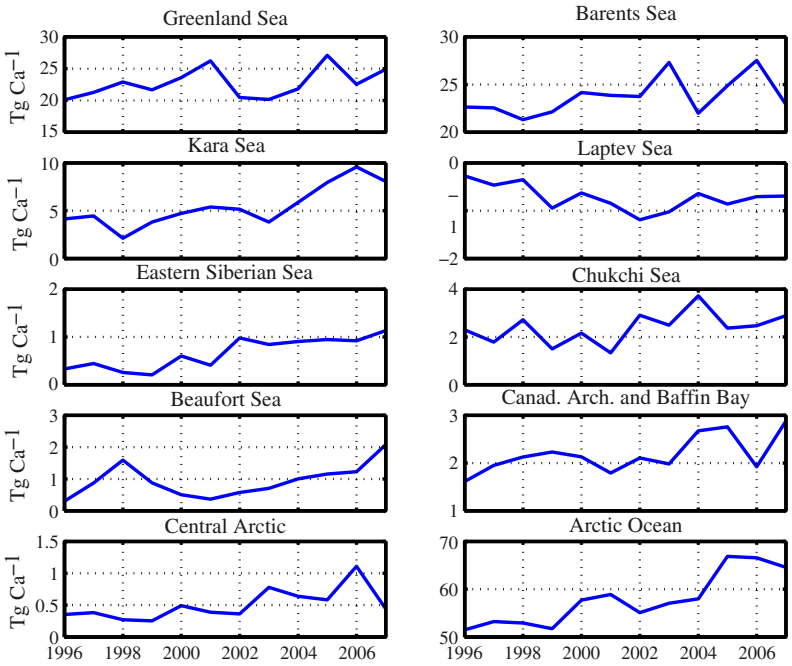

Figure 6. Temporal evolution of annual average of air-sea CO_2 fluxes in the nine selected sectors and in the Arctic Ocean computed by the biogeochemical model for the period 1996–2007. Units are Tg C a^{-1}, and positive values indicate CO_2 uptake.

the efficiency of the biological pump that is favored by more areas of open water.

[28] This enhanced biological pump overcomes the reduction of the efficiency of the solubility pump due to the increase in SST from 2004 to 2005. With a further reduction in sea ice area from 2006 to 2007, however, the enhancement of the biological pump is not enough to counteract the solubility effect that lowers the capacity for CO_2 uptake of the entire Arctic Ocean.

[29] We computed the anomalies of SST, sea ice area, and ocean CO_2 sink for 2005 and 2007 subtracting from the annual average of each of these diagnostics the average value for the 1996–2007 period. As expected, the East Siberian and Chukchi Seas show signs of change although they reveal, on annual average, anomalies of both ingassing and outgassing in correspondence to areas of reduction of sea ice area (Figure 7, middle panels) that mainly correspond to warming SST anomalies (Figure 7, top panels). The anomalies in the East Siberian and Beaufort Seas correspond to an enhancement of the CO_2 uptake while the Chukchi Sea shows a CO_2 outgassing anomaly close to the Bering Strait and a CO_2 uptake anomaly on the shelf area inside the Arctic Ocean (Figure 7, bottom panels).

[30] In 2005, the Kara Sea, part of the Barents Sea, and the Greenland Sea show a positive anomaly of the CO_2 sink indicating an enhanced CO_2 uptake for that year. The rest of the Barents Sea, however, shows an anomaly of CO_2 outgassing for the same year.

[31] In 2007, ingassing and outgassing anomaly patterns are similar to 2005 although the East Siberian Sea outgassing anomaly is larger (Figure 7, bottom panels) showing that the anomaly of the solubility pump dominates over the anomaly associated to the biological pump associated with sea ice area reduction. The outgassing anomaly in the Barents Sea, however, becomes larger, and the CO_2 ingassing area expands in the Greenland Sea too.

[32] These anomalies then would explain why in 2007, although the sea ice area was less than in 2005, the CO_2 sink is not the largest value of the simulated period. In fact, these results would also highlight the importance of the Barents Sea and solubility processes at regulating the basin-scale Arctic Ocean CO_2 sink. Nevertheless, this difference at basin scale should be treated with caution given that the sea ice area minimum in 2007 was underestimated by our sea ice model.

[33] The decomposition of the different components of the surface ocean pCO_2 gave us important information on the role of the solubility and the biological pumps and their temporal changes. However, no information was provided on the role of vertical mixing (and its temporal changes) at driving the changes in surface ocean pCO_2 and hence CO_2 sink of the Arctic Ocean. In order to indirectly address the role of physical ventilation, we show the temporal evolution of the mixed layer depth (MLD; in this case, we approximate the planetary boundary layer computed by our model according to *Large and Yeager* [2004] to the oceanic mixed layer depth) in all the sectors of the Arctic Ocean (Figure 8). For some sectors of the Arctic Ocean, especially in the final part of our simulation (2004–2007), the progressive reduction of the sea ice area is accompanied by a deepening of the MLD, especially for the entire Arctic Ocean (Figure 8, right, fifth panel). This would suggest that the decrease in sea ice cover would cause a MLD deepening (via wind-driven mixing) that would in theory promote the entrainment of DIC-rich water into the upper ocean and hence lower the potential CO_2 uptake of the

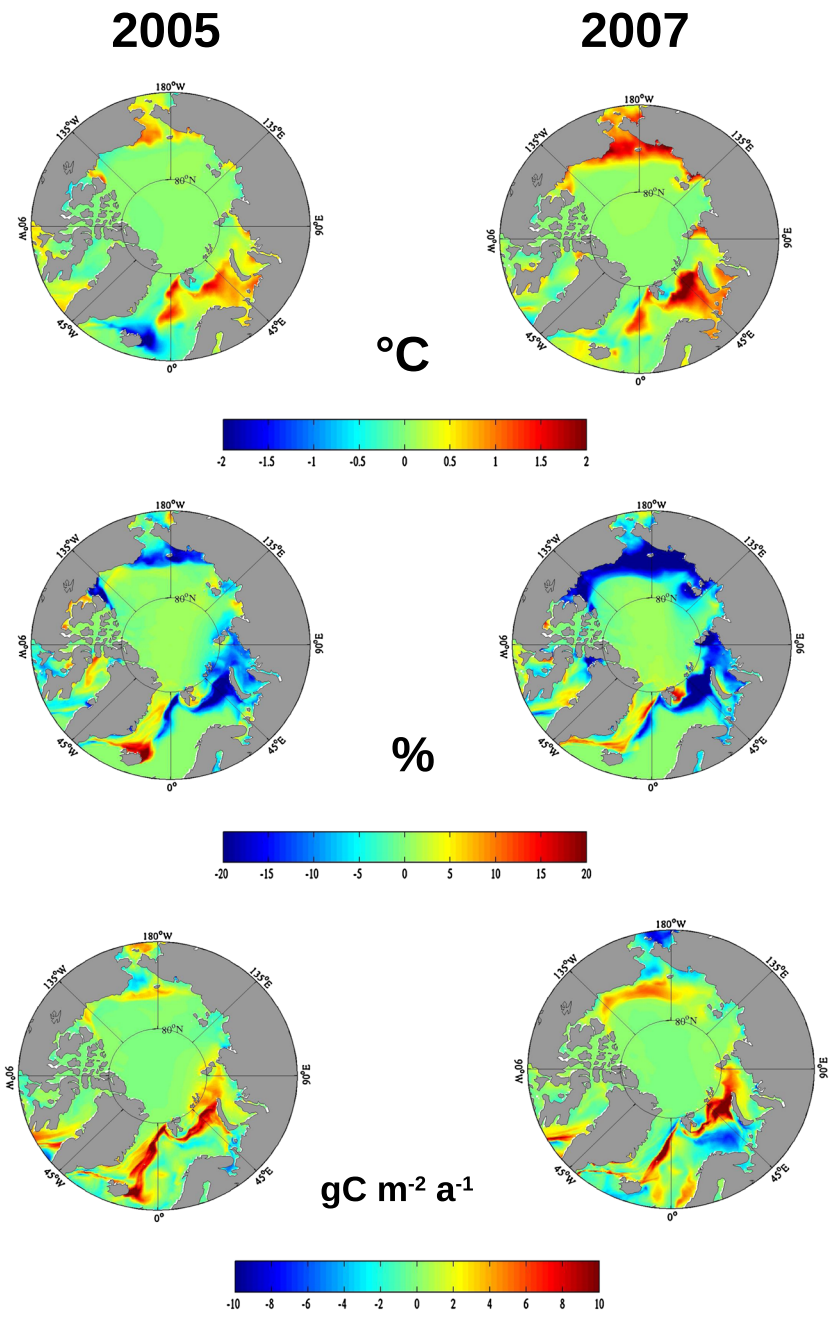

Figure 7. Anomalies of annual mean (top) SST, (middle) sea ice area, and (bottom) CO_2 air-sea fluxes for year (left) 2005 and (right) 2007. Units are from top to bottom °C, percent, and gC m^{-2} a^{-1}, respectively.

Arctic Ocean. However, the progressive decrease in surface ocean pCO_2 (Figure 5, right, fifth panel) and the progressive increase in CO_2 uptake (Figure 6, right, fifth panel) shown by our model would suggest that the effect of increased vertical mixing would be a second order effect while the enhancement of the biological carbon pump would be the dominant mechanism driving ocean CO_2 uptake by the Arctic Ocean.

[34] Furthermore, in order to quantify the difference in carbon uptake in the Arctic Ocean due to the effect of increasing concentration of carbon dioxide, we carried out a second simulation where we kept fixed at 354 ppm, the value corresponding to the average of year 1992, the initial date of our numerical experiments. The comparison of the two different simulations (results not shown here) reveals that first, the difference in carbon uptake for each year is almost negligible and second, that therefore the changes due to the variation of sea ice area are more important than the increase in atmospheric CO_2 per se to drive the interannual changes in carbon uptake of the Arctic Ocean.

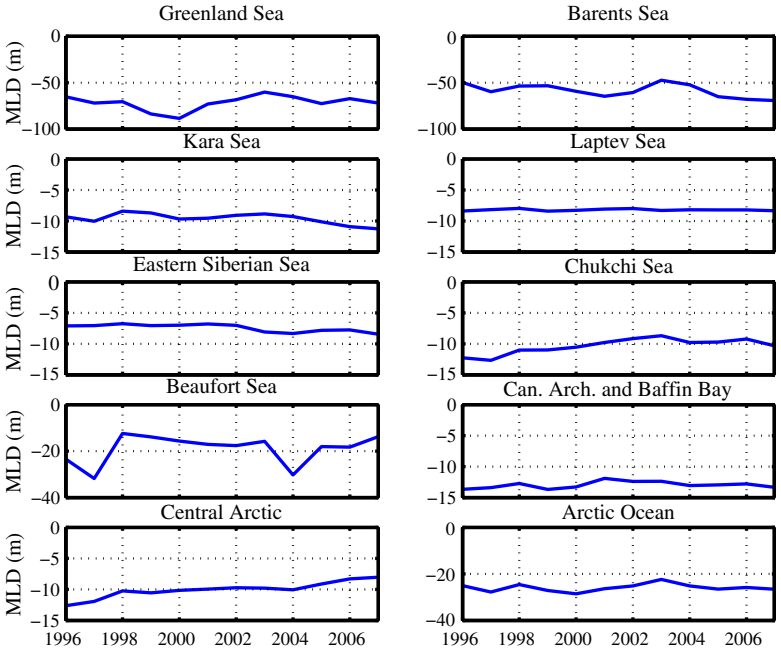

Figure 8. Temporal evolution of annual average of the mixed layer depth in the nine selected sectors and in the Arctic Ocean computed by the physical ocean model for the period 1996–2007. Units are meters.

4. Discussion and Conclusions

[35] We have used a physical-biogeochemical model of the Arctic Ocean forced by the NCEP/NCAR atmospheric reanalysis in order to explore the mechanisms behind the recent changes in the ocean CO_2 sink for a period (1996–2007) characterized by drastic sea ice area reduction. The results show increasing sea surface temperature (SST, Figure 2) and decreasing sea ice area (Figure 3) consistent with observations although with some discrepancies. The progressive sea ice area reduction promotes a marked increase in the simulated productivity that is consistent with satellite-derived estimates of primary production for those waters. This promotes a larger oceanic CO_2 sink due to larger areas of the ocean available for biological drawdown of DIC.

[36] New ice-free areas, however, experience warmer SST, which partially offsets the increased biological sink of CO_2. Our estimates are within the range proposed by previous studies based on in situ oceanic observations and on satellite retrievals. *Bates et al.* [2006] estimated that during the last three decades, the Arctic Ocean increased its CO_2 sink by 24 to 66 Tg C a^{-1}. This implies that the CO_2 sink increased at a rate of 1.4 Tg C a^{-1}. For the 1996–2007 period, this model estimates a time-mean CO_2 sink of 58 Tg C a^{-1}, which increases at a rate of 1.4 Tg C a^{-1}. Both the time-mean and the rate of increase of the simulated CO_2 sink are consistent with the estimates of *Bates et al.* [2006] and with a more recent budget with a higher upper limit (66–199 Tg C a^{-1}) proposed by *Bates and Mathis* [2009].

[37] *Arrigo et al.* [2011] proposed an estimate of 137 Tg C a^{-1} for the months when the sea ice is melting (April to September). It is interesting to note that in the study of *Arrigo et al.* [2011], the mean values of the Eurasian areas are remarkably larger than our estimates. They reported estimates of ocean CO_2 uptake of 12±3.5 Tg C a^{-1} for the Kara Sea, 9.6±3.5 Tg C a^{-1} for the Laptev Sea, and 5.6±2 Tg C a^{-1} for the East Siberian Sea while for the same areas our simulation results are 5.4±2.1, –0.7±0.2 (ocean CO_2 outgassing), and 0.6±0.3 Tg C a^{-1}, respectively (Table 1). This large discrepancy in the Laptev Sea may be due to the fact that *Arrigo et al.* [2011] excluded the nearshore values of DIC in their diagnostic methodology, while we explicitly modeled the influence of remineralized carbon of terrestrial origin in coastal waters. As a direct consequence of this land-ocean coupling, simulated surface ocean pCO_2 [*Manizza et al.*, 2011] in proximity to the Siberian river mouths is substantially larger (by 100–150 μatm) than those reported for these shelf regions by *Arrigo et al.* [2011]. The estimates of ocean CO_2 sink and of surface ocean pCO_2 derived in this study for these three regions are more consistent with those reported by *Bates and Mathis* [2009], which are based on in situ observations, suggesting that the explicit modeling of this biogeochemical mechanism is an important component of the Arctic Ocean carbon cycle.

Table 1. Summary of CO_2 Sink for the Different Sectors of the Arctic Ocean and Their Relative Area[a]

Sector	Area (10^6 km^2)	CO_2 Sink (Tg C a^{-1})
Greenland Sea	2.3	23±2.3
Barents Sea	1.4	24±1.2
Kara Sea	1.3	5.4±21.
Laptev Sea	1.0	-0.7±0.2
East Siberian Sea	1.0	0.6±0.3
Chukchi Sea	0.95	2.3±0.6
Beaufort Sea	1.1	0.9±0.5
Can. Arch. and Baffin Bay	2.0	2.2±0.3
Central Arctic	2.4	0.5±0.2
Arctic Ocean	13.4	58.2±6

[a]Positive values indicate ocean CO_2 uptake.

[38] We also report a discrepancy in the Canadian Archipelago-Baffin Bay and Central Arctic sectors between our estimates and those proposed by *Bates and Mathis* [2009]. For these regions, it is extremely difficult to have a meaningful comparison because of the severe lack of data. In fact, *Bates and Mathis* [2009] proposed estimates based on either a very limited data set (Central Arctic) or on extrapolations based on estimates for the adjacent Beaufort Sea. For the Beaufort Sea, our estimates (0.9 ± 0.5 Tg C a^{-1}) are relatively close to those proposed by *Bates and Mathis* [2009] (2 Tg C a^{-1}) but smaller than those worked out by *Arrigo et al.* [2011] (10 Tg C a^{-1}). For the Chukchi Sea, the estimates proposed by *Bates and Mathis* [2009] (11–53 Tg C a^{-1}) are far greater than in this study (2.3 Tg C a^{-1}) or than *Arrigo et al.* [2011] (9.6 Tg C a^{-1}).

[39] Our model results suggest that the generally held view that a reduced sea ice area would directly translate into lager CO_2 sink is not always correct. *Slagstad et al.* [2011] proposed that a future ice-free Arctic will increase its basin-scale production. The potential mismatch between the response of ocean productivity and ocean carbon sink to the same event of drastic sea-ice loss can be due to the complex response of the upper ocean carbon chemistry, which also depends on the changes in temperature and salinity [*Zeebe and Wolf-Gladrow*, 2003]. In fact, the maximum oceanic CO_2 sink occurs in 2005 and not in 2007 even though sea ice area is lower in 2007 than in 2005.

[40] Although the simulation results obtained in this study show values of CO_2 sink mostly comparable to other independent observation-based studies, the following caveats must be kept in mind.

[41] First, our model also uses PO_4 as the only limiting nutrient although field data would suggest that nitrogen is the major limiting nutrient for Arctic Ocean productivity [*Tremblay et al.*, 2006]. Our choice was dictated by the fact that using PO_4 would avoid the full representation of the ocean nitrogen cycle including the processes of both denitrification and nitrogen fixation. In the Arctic Ocean, most of denitrification occurs in the sediments of the continental shelves [*Devol et al.*, 1996] and given that we did not include in our model any sedimentary compartment we could not have any representation of this process in our study. Nevertheless, the model adopts Redfield ratio assuming that changes in the nitrogen pool are mirrored by the phosphorus pool.

[42] Second, the biogeochemical model used for this study lacks a complete representation of the ecosystem dynamics and explicit plankton functional types that can have a different response to ocean climate warming, with potential consequences for the export of carbon and hence the CO_2 sink [*Bopp et al.*, 2005; *Li et al.*, 2009; *Manizza et al.*, 2010; *Follows and Dutkiewicz*, 2011]. The observed and simulated SST warming trend, if continuing, could potentially influence the metabolism of planktonic organisms, boosting the processes of both photosynthesis (and hence primary production) [*Eppley*, 1972; *Antoine and Morel*, 1996] and heterotrophic respiration. This could then generate potential shifts in the current metabolic state of the Arctic Ocean with important implications for carbon uptake.

[43] Third, the model-data comparison relative to sea ice area shown in section 3.1 indicated that our model overestimates the amount of sea ice area in most of the regions of the Arctic Ocean when compared to satellite-derived data. This bias would imply that our biogeochemical model also underestimates the CO_2 sink of the Arctic Ocean for the simulated period. Nevertheless, we have also shown in our study that the interplay between sea ice reduction and SST warming is more important than simple sea ice reduction in driving the total CO_2 sink of the Arctic Ocean. Furthermore, as previously shown in section 3.1, the major difference between model and data of sea ice area (not shown here) is the timing of spring melting [*Nguyen et al.*, 2011] that could potentially impact the seasonal cycle of NCP , surface nutrient exhaustion, and hence the ocean CO_2 uptake due to action of the biological pump. Although the sea ice concentration bias should be kept in mind, the main results of this study pertain to the complex interplay of multiple processes responsible for driving air-sea CO_2 exchange in the Arctic Ocean. The same principle could be also valid for the SST model-data mismatch that would impact the efficiency of the solubility pump and its temporal variability. In fact, if our model shows an underestimation of the SST at basin scale (Figure 2, right, bottom panel), one should bear in mind that our model is also likely to overestimate the strength of the solubility pump of the Arctic Ocean in our numerical simulations.

[44] Fourth, the Arctic Ocean, especially in the Eurasian shelf and in the Central Arctic, is poorly covered with observations, both physical and biogeochemical, so that it is difficult to evaluate model results, especially during winter months.

[45] Fifth, the particular ocean and sea ice model configuration that we used for this study had not yet been adjusted to represent ocean circulation and sea ice area as accurately as done in *Nguyen et al.* [2011]. In particular, this simulation has more sea ice area that the observed 2007 minimum, which impacts estimates of Arctic Ocean CO_2 sink.

[46] Although the results presented herein can be improved in many ways, they nevertheless provide a sensitivity study for the possible future response of the Arctic Ocean to increased atmospheric CO_2 concentration and associated warming. Some of the state-of-the-art coupled climate models predict that in a few decades the Arctic could be completely ice free during the summer [*Holland et al.*, 2006]. This scenario implies a potential increase in oceanic CO_2 uptake in this region, although many different and competing processes might occur at the same time, as shown in this study.

[47] A factor that can slow down a progressive CO_2 uptake would be the exhaustion of macronutrients in the euphotic zone. In our study, none of the sectors of the Arctic Ocean experienced phosphate limitation (not shown here) in spite of the progressive increase in the activity of the biological pump. Nutrient depletion is more likely to happen on the Eurasian Shelves and in the Central Arctic Ocean, where concentrations are lower than in the Western sector due to influx of waters of Pacific origin through the Bering Strait [*Bates*, 2006].

[48] *Slagstad et al.* [2011] showed that in the East Siberian Sea, the more drastic scenario of sea ice area reduction could reduce the amount of nitrate but not yet to cause a total depletion in the euphotic zone. Their results, however, were obtained from 4 year simulations where the long-term effect of that climatic state could not be realistically explored. In an ice-free Arctic Ocean during summer, some

areas could experience an unprecedented and intensified wind-driven mixing that could replenish the mixed layer with nutrients [*Carmack and Chapman*, 2003] and sustain primary production for periods longer than current climate conditions.

[49] *Vaquer-Sunyer et al.* [2010] showed that the respiration rate of planktonic communities responds to increased temperature more markedly during spring and summer than during winter. Spring and summer are the periods when the sea ice melts and the Arctic Ocean normally takes up CO_2 from the atmosphere, suggesting that the water temperature increase could be an important factor for the future metabolic state of the Arctic Ocean. Furthermore, *Kritzberg et al.* [2010] showed that large increases in water temperature can impact the balance of processes carried out by Arctic marine bacteria. These recent results would suggest that in order to correctly predict the future carbon sink of the Arctic Ocean, ocean biogeochemical models should include these processes with explicit planktonic and bacterial dynamics.

[50] In our simulation, we imposed the same seasonal cycle of biogeochemical properties for each simulated year at both Pacific and Atlantic open boundaries. The biogeochemical changes of the future Arctic Ocean could also depend on the impact of anthropogenic climate change influencing the biogeochemical processes upstream of the Arctic in the subpolar North Atlantic and Pacific Oceans. For instance, the strengthening of biological pump in the subpolar North Pacific due to ocean climate warming [*Bopp*, 2001; *Sarmiento et al.*, 2004] might cause a reduction in the flow of macronutrients through the Bering Strait that normally supports the ecosystems of the Chukchi Sea, Beaufort Sea, Canadian Archipelago, and down to Baffin Bay.

[51] The future development and use of complex ocean ecosystem-biogeochemical models embedded in high-resolution ocean circulation models is critical to understand and quantify the impact of climate change on the complex interactions that regulate the biogeochemical functioning, not only of the Arctic Ocean but also of the subarctic regions of the Atlantic and the Pacific Oceans, which are interconnected through this key polar region.

[52] **Acknowledgments.** This work is a contribution to the ECCO2 project sponsored by the NASA Modeling Analysis and Prediction (MAP) program and to the "Synthesis of the Arctic System Science" project funded by the National Science Foundation. M.M. and M.J.F. were financially supported by the NSF grant ARC-0531119 and SD by NOAA grant NA09OAR4310069. M.M. thanks the NASA AMES Research Center for computer time and technical support when carrying out numerical simulations and the Scripps Institution of Oceanography postdoctoral program for additional financial support while completing the manuscript. We also thank Nick Bates and Jeremy Mathis for helpful discussions.

References

Antoine, D., and A. Morel (1996), 1. Adaptation of a spectral light-photosynthesis model in view of application to satellite chlorophyll observations, *Global Biogeochem. Cycles*, *10*(1), 43–55.

Arrigo, K., G. van Dijken, and S. Pabi (2008), Impact of a shrinking Arctic ice cover on marine primary production, *Geophys. Res. Lett.*, *35*, L19603, doi:10.1029/2008GL035028.

Arrigo, K., S. Pabi, G. van Dijken, and W. Maslowski (2011), Air-sea flux of CO_2 in the Arctic Ocean, 1998-2003, *J. Geophys. Res.*, *115*, G04024, doi:10.1029/2009JG001224.

Bates, N. R. (2006), Air-sea CO_2 fluxes and the continental shelf pump of carbon in the Chuckchi Sea adjacent to the Arctic Ocean, *J. Geophys. Res.*, *111*, C10013, doi:10.1029/2005JC003083.

Bates, N. R., and J. T. Mathis (2009), The Arctic Ocean marine carbon cycle: Evaluation of air-sea CO_2 exchanges, ocean acidification impacts and potential feedbacks, *Biogeosciences*, *6*(11), 2433–2459, doi:10.5194/bg-6-2433-2009.

Bates, N. R., S. D. Moran, D. A. Hansell, and J. T. Mathis (2006), An increasing CO_2 sink in the Arctic Ocean due to the sea-ice loss, *Geophys. Res. Lett.*, *33*, L23609, doi:10.1029/2006GL027028.

Bopp, L. (2001), Changements climatiques et biogéochemie marine: Modelisation du dernier maximum glaciaire et de l'Ére industrielle, Ph. D. thesis, Université Paris VI.

Bopp, L., O. Aumont, P. Cadule, S. Alvain, and M. Gehlen (2005), Response of diatoms distribution to global warming and potential implications: A global model study, *Geophys. Res. Lett.*, *32*, L19606, doi:10.1029/2005GL023653.

Carmack, E., and D. C. Chapman (2003), Wind-driven shelf/basin exchange on an Arctic shelf: The joint roles of ice cover extent and shelf-break bathymetry, *Geophys. Res. Lett.*, *30*(14), 1778, doi:10.1029/2003GL017526.

Comiso, J., D. Cavalieri, C. Parkinson, and P. Gloersen (1997), Passive microwave algorithms for sea ice concentration: A comparison of two techniques, *Remote Sens. Environ.*, *60*, 357–384.

Condron, A., P. Winsor, C. N. Hill, and D. Menemenlis (2009), Response of the Arctic freshwater budget to extreme NAO forcing, *J. Clim.*, *22*, 2422–2437.

Devol, A. H., L. Codispoti, and J. P. Christensen (1996), Summer and winter denitrification rates in western Arctic shelf sediments, *Cont. Shelf Res.*, *17*(9), 1029–1050.

Eppley, R. W. (1972), Temperature and phytoplankton growth in the sea, *Fish. Bull.*, *70*, 1063–1085.

Follows, M. J., and S. Dutkiewicz (2011), Modeling diverse communities of marine microbes, *Annu. Rev. Mar. Sci.*, *3*, 427–451.

Follows, M. J., S. Dutkiewicz, S. Grant, and S. W. Chisolm (2007), Emergent biogeography of microbial communities in a model ocean, *Science*, *315*, 1843–1846.

Garcia, H. E., R. A. Locarnini, T. P. Boyer, and J. I. Antonov (2006), *World Ocean Atlas 2005, Volume 4: Nutrients (Phosphate, Nitrate, Silicate), NOAA Atlas NESDIS 64 64*, U.S. Government Printing Office, Washington, D.C.

Giles, K. A., S. W. Laxon, and A. L. Ridout (2008), Circumpolar thinning of arctic sea ice following the 2007 record ice extent minimum, *Geophys. Res. Lett.*, *35*, L22502, doi:10.1029/2008GL035710.

Gouretski, V. V., and K. P. Koltermann, (2004), WOCE global hydrographic climatology, *Technical Report 35*, Berichte des Bundesamtes für Seeschifffahrt und Hydrographie.

Heimbach, P., D. Menemenlis, M. Losch, J.-M. Campin, and C. Hill (2010), On the formulation of sea-ice models. Part 2: Lessons from multi-year adjoint sea ice export sensitivities through the Canadian Arctic Archipelago, *Ocean Modell.*, *33*, 145–158.

Holland, M., C. M. Bitz, and B. Tremblay (2006), Future abrupt reductions in the summer Arctic sea ice, *Geophys. Res. Lett.*, *33*, L23503, doi:10.1029/2006GL028024.

Kahru, M., V. Brotas, M. Manzano-Sarabia, and B. G. Mitchell (2011), Are phytoplankton blooms occurring earlier in the Arctic?, *Global Change Biol.*, *17*, 1733–1739.

Kalnay, E., et al. (1996), The NCEP/NCAR 40-year reanalysis project, *Bull. Am. Meteorol. Soc.*, *77*, 437–471.

Kritzberg, E., C. M. Duarte, and P. Wassmann (2010), Changes in Arctic marine bacterial carbon metabolism in response to increasing temperature, *Polar Biol.*, *33*, 1673–1682.

Large, W. G., and S. G. Yeager, (2004), Diurnal to decadal global forcing for ocean and sea-ice models: The data sets and flux climatologies, *Note tn-460+str*, NCAR, Boulder, CO.

Lauderdale, J. M., A. C. N. Garabato, K. I. C. Oliver, M. J. Follows, and R. G. Williams (2013), Wind-driven changes in Southern Ocean residual circulation, ocean carbon reservoirs and atmospheric CO_2, *Clim. Dyn.*, *41*(7-8), 2145–2164, doi:10.1007/s00382-012-1650-3.

Le Quéré, C., O. Aumont, P. Monfray, and J. Orr (2003), Propagation of climatic events on ocean stratification, marine biology, and CO_2: Case studies over the 1979–1999 period, *J. Geophys. Res.*, *108*(C12), 3375, doi:10.1029/2000IJC000920.

Li, W. K. W., F. A. McLaughlin, C. Lovejoy, and E. C. Carmack (2009), Smallest algae thrive as the Arctic freshens, *Science*, *326*, 539.

Losch, M., D. Menemenlis, P. Heimbach, J.-M. Campin, and C. Hill (2010), On the formulation of sea-ice models. Part 1: Effects of different solver implementations and parameterizations, *Ocean Modell.*, *33*, 129–144.

Manizza, M., M. J. Follows, S. Dutckiewicz, J. W. McClelland, D. Menemenlis, C. N. Hill, A. Townsend-Small, and B. J. Peterson (2009), Modeling transport and fate of riverine dissolved organic carbon in the Arctic Ocean, *Global Biogeochem. Cycles*, *23*, GB4006, doi:10.1029/2008GB003396.

Manizza, M., E. T. Buitenhuis, and C. Le Quéré (2010), Sensitivity of global ocean biogeochemical dynamics to ecosystem structure in a future climate, *Geophys. Res. Lett.*, *37*, L13607, doi:10.1029/2010GL043360.

Manizza, M., M. J. Follows, S. Dutkiewicz, J. W. McClelland, D. Menemenlis, C. N. Hill, B. J. Peterson, and R. M. Key (2011), A model of the Arctic Ocean carbon cycle, *J. Geophys. Res.*, *116*, C12020, doi:10.1029/2011JC006998.

Marshall, J., C. Hill, L. Perelman, and A. Adcroft (1997), Hydrostatic, quasi-hydrostatic and nonhydrostatic ocean modeling, *J. Geophys. Res.*, *102*(C3), 5,733–5,752.

McGuire, A. D., L. G. Anderson, T. R. Christensen, S. Dallimore, L. Guo, D. J. H. M. Heimann, T. D. Lorenson, R. W. Macdonald, and N. Roulet (2009), Sensitivity of the carbon cycle in the Arctic to climate change, *Ecol. Appl.*, *79*(4), 523–555.

McKinley, G., M. J. Follows, and J. C. Marshall (2004), Mechanisms of air-sea CO_2 flux variability in the equatorial Pacific and in the North Atlantic, *Global Biogeochem. Cycles*, *18*, GB2011, doi:10.1029/2003GB002179.

McKinley, G. A., et al. (2006), North Pacific carbon cycle response to climate variability on seasonal to decadal timescales, *J. Geophys. Res.*, *111*, C07S06, doi:10.1029/2005JC003173.

Nguyen, A. T., D. Menemenlis, and R. Kwok (2009), Improved modeling of the Arctic halocline with a subgrid-scale brine rejection parameterization, *J. Geophys. Res.*, *114*, C11014, doi:10.1029/2008JC005121.

Nguyen, A. T., D. Menemenlis, and R. Kwok (2011), Arctic ice-ocean simulation with optimized model parameters: Approach and assessment, *J. Geophys. Res.*, *116*, C04025, doi:10.1029/2010JC006573.

Pabi, S., G. L. van Dijken, and K. Arrigo (2008), Primary production in the Arctic Ocean, 1998–2006, *J. Geophys. Res.*, *113*, C08005, doi:10.1029/2007JC004578.

Reynolds, R. W., T. M. Smith, C. Liu, D. B. Chelton, K. Casey, and M. G. Schlax (2007), Daily high-resolution-blended analyses for sea surface temperature, *J. Clim.*, *20*, 5473–5496.

Rodrigues, I. (2008), The rapid decline of the sea ice in the Russian Arctic, *Cold Reg. Sci. Technol.*, *54*, 124–142.

Rothrock, D. A., D. B. Percival, and M. Wensnahan (2008), The decline in arctic sea-ice thickness: Separating the spatial, annual, and interannual variability in a quarter century of submarine data, *J. Geophys. Res.*, *113*, C05003, doi:10.1029/2007JC004252.

Sarmiento, J. L., et al. (2004), Response of ocean ecosystems to climate warming, *Global Biogeochem. Cycles*, *18*, GB3003, doi:10.1029/2003GB002134.

Slagstad, D., I. H. Ellingsen, and P. Wassmann (2011), Evaluating primary and secondary production in an Arctic Ocean void of summer sea ice: An experimental simulation approach, *Prog. Oceanogr.*, *90*, 117–131.

Steele, M., W. Ermold, and J. Zhang (2008), Artic Ocean surface warming trends over the past 100 years, *Geophys. Res. Lett.*, *35*, L02614, doi:10.1029/2007GL0311651.

Stroeve, J., M. M. Holland, W. Meier, T. Scambos, and M. Serreze (2007), Arctic sea ice decline: Faster than forecast, *Geophys. Res. Lett.*, *34*, L09501, doi:10.1029/2007GL029703.

Takahashi, T., et al. (2002), Global sea-air CO_2 flux based on climatological pCO_2, and seasonal biological and temperature effects, *Deep Sea Res. II*, *49*, 1601–1622.

Tremblay, J., C. Michel, K. A. Hobson, M. Gosselin, and N. M. Price (2006), Bloom dynamics in early opening waters of the Arctic Ocean, *Limnol. Oceanogr.*, *5*(2), 900–912.

Vaquer-Sunyer, R., C. M. Duarte, E. Santiago, P. Wassmann, and M. Reigstad (2010), Experimental evaluation of planktonic respiration response to warming in the European Arctic sector, *Polar Biol.*, *33*, 1661–1671.

Verdy, A., S. Dutkiewicz, M. J. Follows, J. C. Marshall, and A. Czaja (2007), Carbon dioxide and oxygen fluxes in the Southern Ocean: Mechanisms of interannual variability, *Global Biogeochem. Cycles*, *21*, GB2020, doi:10.1029/2006GB002916.

Zeebe, R. E., and D. Wolf-Gladrow (2003), *CO_2 in Seawater: Equilibrium, Kinetics, Isotopes, Oceanography*, Elsevier, Amsterdam, The Netherlands.

Zhang, J., and D. Rothrock (2003), Modeling global sea ice with a thickness and enthalpy distribution model in generalized curvilinear coordinates, *Mon. Wea. Rev.*, *131*(5), 681–697.

Zhang, J., Y. H. Spitz, M. Steele, C. Ashajan, R. Campbell, and L. B. P. Matrai (2011), Modeling the impact of declining sea ice on the Arctic marine planktonic ecosystem, *J. Geophys. Res.*, *115*, C10015, doi:10.1029/2009JC005387.